PERGAMON

Vision Research 39 (1999) 901–914

Vision Research

A deficit in strabismic amblyopia for global shape detection

Robert F. Hess [1,2,*], Yi-Zhong Wang [1], Rita Demanins [1], Fran Wilkinson [3], Hugh R. Wilson [4]

[1] *McGill Vision Research, Department of Ophthalmology, McGill University, Montreal, Canada*
[2] *Department of Optometry, Queensland University of Technology, Brisbane, Australia*
[3] *Department of Psychology, McGill University, Montreal, Quebec, Canada*
[4] *Visual Science Center, University of Chicago, Chicago, IL, USA*

Received 12 December 1997; received in revised form 23 April 1998

Abstract

Using a task which relied upon the detection of sinusoidal deformations from circularity, we show that strabismic amblyopes exhibit deficits which are not critically dependent on either the scale of deformation or the spatial frequency characteristics of the stimulus (circular D4) itself. We show that this loss is not due to the restricted passband of the amblyopic eye. Furthermore, in a pedestal distortion experiment, we show that the suprathreshold form of this loss is consistent with an elevated level of 'intrinsic noise' rather than a loss in 'sampling efficiency'. © 1998 Elsevier Science Ltd. All rights reserved.

Keywords: Amblyopia; Shape; Disarray; Undersampling; Distortion; Circularity; Positional uncertainty

1. Introduction

There now seems to be consensus that while there are clear contrast sensitivity deficit in amblyopia, there are others, possibly related to positional uncertainty and/or distortions which are more fundamental. This has been shown in bisection tasks (Bedell & Flom, 1981; Bedell, Flom & Barbeito, 1985), circularity discrimination (Bedell & Flom, 1981; Lagreze & Sireteanu, 1991), vernier alignment (Bedell & Flom, 1981; Levi & Klein, 1982), the alignment of well separated elements (Fronius & Sireteanu, 1989) or Gabors (Hess & Holliday, 1992; Demanins & Hess, 1996) and contour integration (Hess, McIlhagga & Field, 1997). This deficit does not follow as a consequence of the concomitant contrast sensitivity deficit (and appears to be scale invariant and to be largely confined to central vision (Fronius & Sireteanu, 1989; Demanins & Hess, 1996). Ideally the next step is to quantify this spatial disturbance within the framework of how the normal visual system encodes space.

Three decades of neurophysiology have led to the understanding that cells in the primary visual cortex have different spatial, temporal, orientation and contrast filtering properties. This is the obvious place to look for the spatial filtering deficit in amblyopia and there is evidence that high spatial frequency cells driven by the amblyopic eye have reduced contrast sensitivity (Chino, Shansky, Jankowski & Banser, 1983; Crewther & Crewther, 1990). There is now some evidence that the receptive field arrangement of cells in V1 and V4 differ. Linear gratings which have been the stimulus of choice in V1 have been reported to be less effective in driving cells in V4 (Gallant, Braun & Van Essen, 1993; Gallant, Connor, Rakshit, Lewis & Van Essen, 1996). Stimuli with circular structure are more effective, suggesting that the linear receptive fields of V1 may undergo a non-linear transformation and are organized into different spatial configurations in higher visual areas to better encode the global shape of objects. Psychophysical evidence for the existence of units that pool orientation subunits concentrically in human vision has recently been reported (Wilson, Wilkinson & Asaad, 1997). Thus, there is now evidence that the human

* Corresponding author. E-mail: rhess@bradman.vision.mcgill.ca.

PII: S0042-6989(98)00157-6

visual system contains global form units like those reported by Gallant et al. (1993, 1996) in primate V4 which underlie our high sensitivity for detecting subtle changes in the circular shape of objects (Wilkinson, Wilson & Habak, 1998).

There have been two suggestions proposed for the positional uncertainty in amblyopia which is particularly evident using stimuli thought to be processed by non-Fourier mechanisms (Hess & Holliday, 1992; Demanins & Hess, 1996): undersampling and topological disarray. Either of these if applied to V1 would disrupt circularly arranged receptive fields in higher visual areas and would be expected to produce a performance deficit for encoding global shape. However the type of performance deficit may well tell us not only where in the visual system the spatial deficit occurs but also what type of deficit it is.

Consider the undersampling proposal. If the undersampling is at an early level in the visual system (i.e. V1 afferents or V1 cells) then circularity detection should be normal for spatially narrow-band stimuli that fall well within the systems sampling limit. Thus the abnormality would critically depend on the luminance spatial frequency composition of the stimuli from which circularity is to be gauged. If the undersampling occurs at a higher level where there is a more feature-based representation (Levi & Klein, 1996; Wang, Levi & Klein, 1998) of the stimulus then performance should be normal for low frequency spatial perturbations compared with the sampling limit. In this case, detection abnormalities would be seen for changes in position over small spatial extents (high-frequency space modulations) but not over larger spatial extents (low-frequency space modulations). Topological disarray of a scale invariant form would have somewhat different detection predictions. Its effect would not diminish for either stimuli composed of low luminance spatial frequencies or for stimuli modulated at low space frequencies. Furthermore, the suprathreshold nature of the deficit would be different for undersampling versus topological disarray; spatial undersampling results in a loss of 'sampling efficiency' whereas topological disarray results in a raised level of 'intrinsic noise'. An evaluation of suprathreshold discrimination for these stimuli may allow one to distinguish between these two predictions.

In the present study we measure detection and discrimination performance for sinusoidal perturbations of contours constructed from 4th derivatives of a Gaussian. For normal vision, the threshold for detecting such sinusoidal perturbations is very low (Wilson et al., 1998) and can be modeled on the basis of what is known of the non-Fourier, non-Cartesian cells reported in V4 (Wilson et al., 1997; Wilkinson et al., 1998). Such stimuli have the dual advantage of being spatial frequency narrow-band and having well controlled shape perturbations of different magnitudes or scale.

2. Methods

2.1. Subjects

Ten strabismic amblyopes participated in the study. Table 1 shows the clinical data of all subjects. Subjects wore their spectacle corrections.

2.2. Stimuli

Stimuli were circular 4th derivative of Gaussian (D4) contours (Wilson et al., 1998), which are band-limited (full bandwidth of 1.24 octaves) in the spatial frequency domain (see Fig. 1 for examples). The circular D4 is generated by the following equations:

$$\mathrm{CD4} = L_m\left[1 + c\left(1 - 4r^2 + \frac{4}{3}r^4\right)\mathrm{e}^{-r^2}\right] \quad (1)$$

$$r = \frac{\sqrt{x^2 + y^2} - R}{\sigma} \quad (2)$$

$$\sigma = \frac{\sqrt{2}}{\pi\omega_p} \quad (3)$$

where σ is the space constant of D4, ω_p is the D4 peak spatial frequency, R is the radius of circular D4 contour, which is modulated sinusoidally according to the following formula:

$$R = R_m\left\{1 + A\sin\left[f_r \arctan\left(\frac{y}{x}\right) + \theta\right]\right\} \quad (4)$$

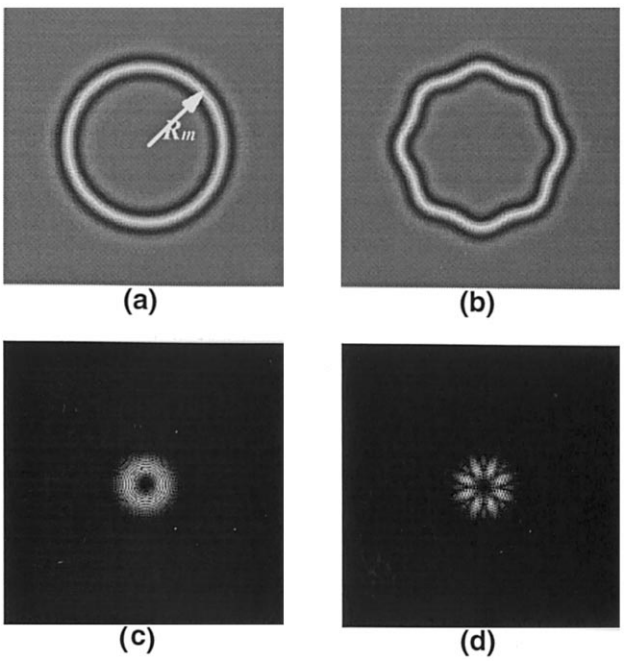

Fig. 1. Examples of stimuli and their amplitude Fourier spectra. (a) unmodulated circular D4 contour; (b) modulated circular D4 contour with radial frequency of 8 cyc/360° and radius modulation of 4%. (c, d) are amplitude spectra of (a, b), respectively.

Table 1
Clinical data for the 10 amblyopic subjects who participated in this study

Subject	Eye	Refraction	Letter acuity	Grating acuity (cyc/°)	Fixation	Ocular alignment	History
BB strab	RE	+0.50/−0.50 × 160	6/5	5	5° nasal	5° LET	Surgery to correct angle of large eso at age 7
	LE	+1.25/−0.25 × 180	6/180				
BC strab/aniso	RE	+2.00/−2.25 × 010	6/15−2	21	Centred	6° RET	Amblyopia diagnosed age 6, Rx for last 12 years, no surgery, no orthoptics
	LE	Plano/−1.25 × 160	6/4.5−2		Centred		
JL strab	RE	+0.75 DS	6/4.5			3° LHT	Initially large eso, orthoptics and surgery age 5
	LE	+0.75/−0.25 × 140	6/30	20	2.5° ecc		
MD strab/aniso	RE	Plano	6/4.5		Centred	8° LET	Diagnosed age 11, patched RE for 1 h/day for 1 year, Rx for 2 years (age 12–14) part time wear only, no surgery
	LE	+3.00 DS	6/24	17	1° nasal		
MJS strab	RE	−1.75/−0.25 × 175	6/4.5		Centered 0.5–1° nasal, unsteady	10° LET	Surgery at age 8
	LE	Plano	6/12+2	28		1° RHT	
MS strab	RE	+0.75 DS	6/6	27	Centred 1° nasal/inf	10° LET	Amblyopia age 9, Rx age 9–20, no patching, no surgery
	LE	+1.00 DS	6/18	27			
OA strab/aniso	RE	−4.50/−5.00 × 030	6/24	13	3° nasal centred	5° RET	Diagnosed age 3, Rx age 3, patching age 3, no surgery
	LE	−1.75/−1.75 × 150	6/6				
RW strab/aniso	RE	+3.50 DS	6/60	15	1° nasal	2° RET	First detected at age 10, no treatment
	LE	−3.00/−1.00 × 120	6/5−1				
SB strab	RE	Plano	6/6	15	Centred	2° LET	Microtropia diagnosed age 4, no treatment
	LE	+0.50 DS	6/60	15	2° nasal		
VE strab/aniso	RE	+0.75 DS	6/6+2		Centred	9° LXT near	LXT diagnosed age 7, Rx since age 7, no patching, no surgery
	LE	+3.00 DS	6/18−2	16	Centred	6° LXT distance	

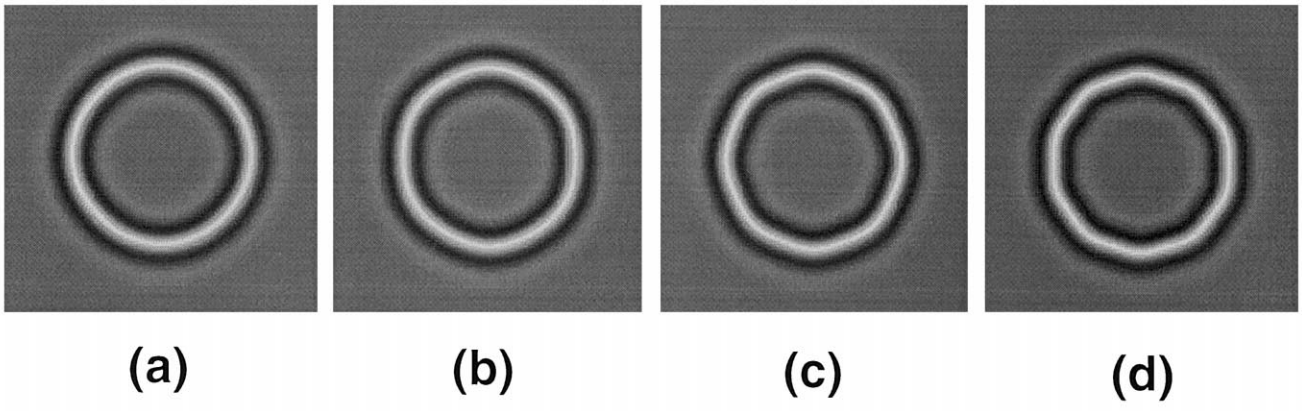

Fig. 2. Examples of stimuli used in this study. At viewing distance of 1.5 m, the D4 peak spatial frequency is 5 cyc/°; the mean radius is 0.5°; amplitude of radial modulation is 1%. Radial frequencies are 4, (a); 6, (b); 8, (c); and 10, (d) cyc/360°, and the modulation phases are 90, 270, 90, and 270°, respectively.

where R_m is the mean radius, f_r is the radial frequency; A is the amplitude of the radial modulation, and θ is the phase of the modulation where $0 < \theta < 2\pi$.

Stimuli were generated digitally in MATLAB (MathWorks) and displayed on a gamma-corrected, Macintosh gray-scale monitor by using the Psychophysics Toolbox (Brainard, 1997) which provides high level access to the C-language VideoToolbox (Pelli, 1997). The mean luminance of the monitor was 20 cd/m^2. The stimulus screen subtended $12 \times 9°$ at the viewing distance of 1.5 m. The mean radius was 0.5°. The radial frequencies were 4, 6, 8, or 10 cyc/360°(see Fig. 2). The phase of radial modulation was chosen so that the circular D4 contour was symmetric about the vertical axis. The D4 peak spatial frequencies were 2.5, 5,10, or 15 cyc/°. The contrast of stimuli ranged from 10 to 80%. Data was collected for a fixed range of D4 peak spatial frequencies which fell within the acuity of the amblyopic eye. In some cases, a range of different D4 peak frequencies were used to examine the effect of this choice.

2.3. Psychophysical procedures

A 2-interval, forced-choice paradigm was employed to estimate the detection and amplitude modulation increment discrimination thresholds of radial frequency modulations for both affected and dominant eyes of amblyopic subjects. For the detection task, one interval in a trial contained an unmodulated circular D4 contour and the other contained a modulated circular D4 contour. Subjects were asked to indicate which interval had the modulated (or non-circular) contour. For the increment discrimination task, both intervals in a trial contained modulated circular D4 contours: one interval with base modulation and the other with base modulation plus increment modulation. Subjects were required to report the interval which had the more distorted circular D4 contour. The data is based on multiple runs and no learning effects were observed even though some subjects were tested over an extensive period.

The location of the stimulus presented on the screen was randomized from trial-to-trial by randomizing the stimulus location using a Gaussian random variable. The S.D. of this Gaussian variable was equal to the mean radius of the circular D4 contour. The duration of each stimulus presentation was 0.5 s. Each session consisted of ten trials for each of five test modulations. Audio signals were used to prompt the subject just before and after each trial, but no feedback about the correctness of responses was provided. For each combination of test radial frequency and D4 peak spatial frequency, psychometric functions of correct response versus test modulation were generated and fit with a Weibull function (Weibull, 1951; Nachmias, 1981). Threshold modulations corresponding to 82% correct were interpolated from the Weibull fits.

Three experiments were carried out. In the first experiment, amblyopic subjects' detection thresholds for radial frequency modulation were measured. The second experiment investigated the effect of stimulus contrast on the detection threshold. The increment threshold for radial frequency modulation was determined in the third experiment.

3. Results

A typical example of the psychometric data for the dominant and amblyopic eye of a strabismic is seen in Fig. 3. Percent correct as a function of modulation amplitude in arc seconds is plotted for a range of radial frequencies for the dominant and amblyopic eye of this subject. The lines are the Weibull fits.

There is a clear difference in the threshold between the dominant and amblyopic eye across a wide range of

radial frequencies (see also Fig. 4, subject MD, where this data is replotted). To a first approximation, the deficit is invariant with radial frequency (i.e. scale invariant) and represents a 5-fold elevation of threshold. It is also apparent that, for the fellow dominant eye, the threshold is quite low (e.g. 3.6 arc s) and does not dramatically vary with radial frequency apart from showing an elevation at the lowest radial frequency.

Results for a group of strabismic amblyopes are shown in Fig. 4 where modulation threshold is plotted against the radial frequency of the D4 circular pattern. All amblyopes were tested with D4 patterns whose peak spatial frequency fell within their spatial pass-band. This ensured that the stimulus itself was always visible and that any performance deficit was due to an inability to detect radial frequency modulations per second. All subjects displayed reduced performance with their amblyopic eyes for detection of radial modulations. What is noteworthy is that this involved even the lowest modulation frequency tested (namely 4 cyc/360°).

Since the D4 contours had a peak spatial frequency of 5 cyc/° and the grating acuity varies for different amblyopic eyes, these results correspond to different ratios of D4 spatial frequency/amblyopic cut-off spatial frequencies. This ratio ranged from unity to a factor of five. To gauge the effect of the composition of the D4 stimulus relative to the amblyopic filtering deficit we measured performance for a range of different ratios of D4 peak spatial frequency/amblyopic acuity in a number of amblyopic observers. Fig. 5 shows two such examples. In these case, four D4 peak frequencies are compared giving ratios from 1.13 to 6.8. It is evident that the closer the D4 peak

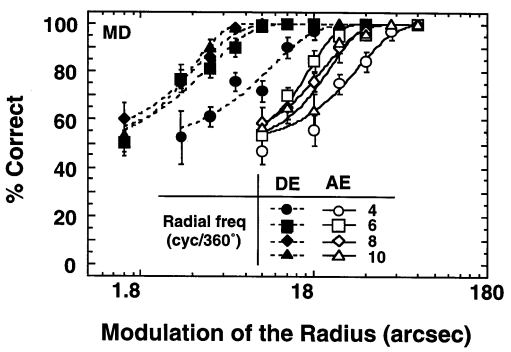

Fig. 3. Examples of psychometric functions for detecting radial modulation obtained from subject MD. The peak spatial frequency of circular D4 contours was 5 cyc/°. Radial frequencies were 4 (circles), 6 (squares), 8 (diamonds), or 10 (triangles) cyc/360°. The mean radius was 0.5°. Closed symbols are the results from the dominant eye, and open symbols are those from the amblyopic eye. Error bars indicate ± S.E.M. of each data point. Detection thresholds corresponding to 82% correct were interpolated from Weibull functions (curves) fit to the data. The error bars are ± S.E.M. of at least five measurements.

frequency is to the subjects cut-off grating acuity, the larger is the deficit for the detection of radial modulations. However this effect is not large (a factor of two averaged across radial frequency) compared to the resident deficit which is still evident at all radial frequencies tested.

These results indicate that the deficit for detection of radial modulations by the amblyopic eye is not simply a consequence of the peak spatial frequency of the D4 stimulus being too close to the cut off spatial frequency of the amblyopic eye. If this were the case, radial modulation threshold for D4 patterns well separated from the grating acuity limit of the amblyopic eye would be unaffected and this is clearly not the case.

Another way of addressing this same issue is to ask 'do comparable radial modulation deficits occur for comparable ratios of D4 peak spatial frequency/cut-off acuity?'. In Fig. 6 two sets of amblyopic radial threshold data are compared for stimulus conditions where the ratio between the peak spatial frequency of the D4 pattern and the amblyopic cut-off acuity is constant. In A and B, the ratio for these two subjects is fixed at approximately 5, whereas in C and D, it is fixed at approximately 2.5. The resultant deficit for the detection of radial frequencies is clearly not dependent on just this ratio as the deficit is seen to vary between the two subjects' data.

Another issue related to the visibility of these D4 patterns is whether the known contrast sensitivity deficit exhibited by amblyopic subjects could contribute in part or whole to reduced performance for detecting radial modulations (Fig. 4). It is known that contrast does not critically influence the radial modulation threshold of normal observers (Wilkinson et al., 1998). Fig. 7 shows results for two amblyopes where the contrast of the D4 pattern is varied. The deficit for the detection of radial modulation is not dependent on the contrast of the D4 pattern in the range tested.

An issue of some relevance as to whether these detection deficits for D4 radial modulations are due to a spatial disarray or spatial undersampling concerns the nature of the suprathreshold deficit. To assess this we measured the incremental threshold for radial modulations in a number of amblyopic eyes at representative radial frequencies.

These are plotted as incremental modulation threshold versus base or pedestal modulation in Fig. 8. In all cases, the initial deficit at low base modulations, disappears at high base modulations. At large base modulations, the normal and amblyopic eyes have similar incremental thresholds. All subjects reported that at zero base modulation which corresponds to detection threshold, the unmodulated reference stimulus appeared distorted.

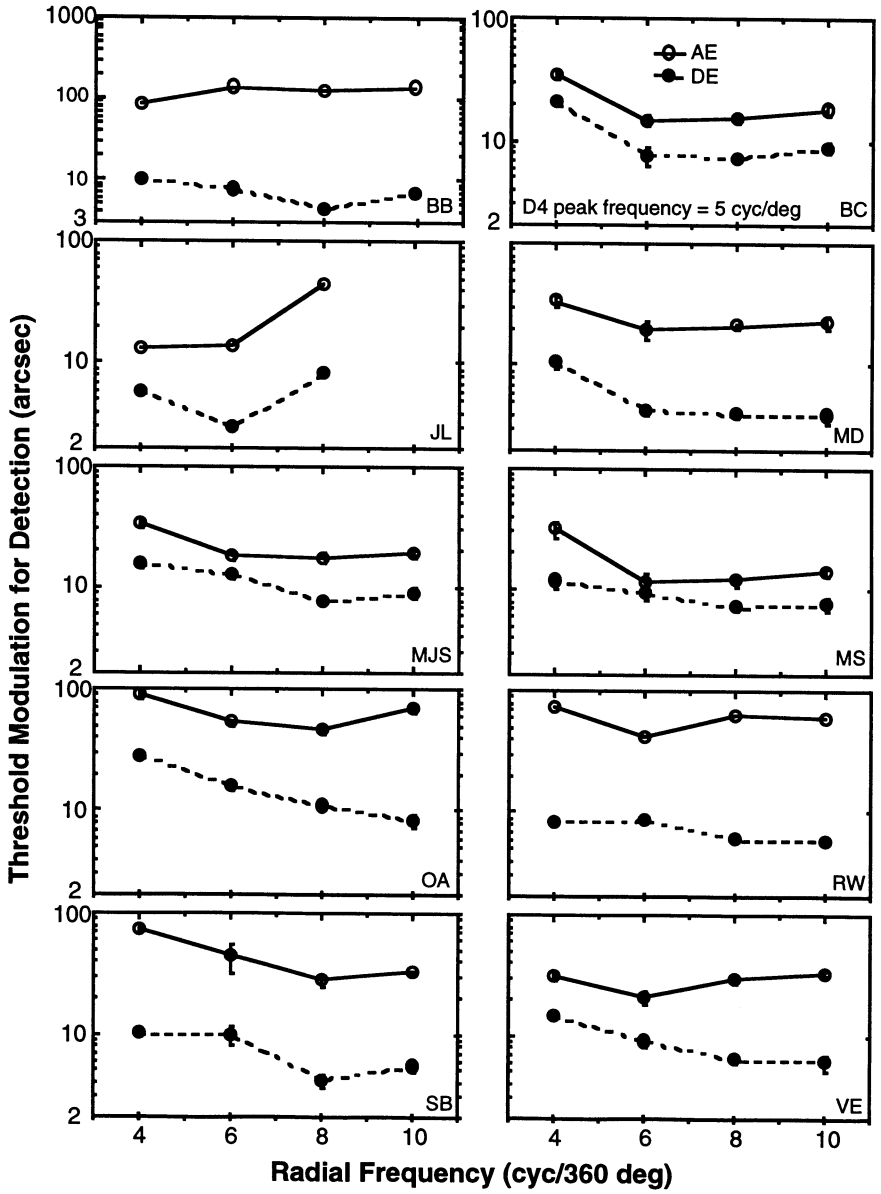

Fig. 4. Threshold modulation for detecting the deformation of circular D4 contours as a function of radial frequency obtained from ten strabismic amblyopes. The peak spatial frequency of circular D4 contours was 5 cyc/°. The mean radius was 0.5°. Closed circles are the results from the dominant eye, and open circles are those from the amblyopic eye. Error bars indicate ±S.E.M. of at least three measurements.

4. Part II modeling

In an effort to illustrate some of the concepts already discussed we produced model reconstructions of our stimuli under conditions of filtering, neural disarray and undersampling. In the case of filtering, D4 patterns were subjected to various degrees of Gaussian low-pass filtering. In the case of neural disarray and undersampling, since these were modelling postreceptoral processes, the stimulus was first convolved with an array of balanced DOG filters which were tuned to the D4 stimulus (sampled convolution-see appendix). Because discrete sampling was used, this is an inherently nonlinear process. Images were reconstructed by adding up all the filters at their respective activities for a particular image.

4.1. Spatial filtering

The influence of spatial filtering is seen in Fig. 9. A deformed D4 pattern whose peak spatial frequency was 5 cyc/° (spectrum shown in Fig. 9(b)) was filtered with a Gaussian low-pass filter with cut-offs from 20 to 5 cyc/°. Even when the cut-off matches the peak spatial frequency of the D4 stimulus, although the contrast of the D4 pattern is reduced there is little or no disruption to the radial modulation. This helps to explain why the spatial filtering deficit in amblyopia would not be ex-

pected to impair performance on our radial modulation task even if the cut off of the amblyopic eye was similar to the spatial frequency composition of the D4 stimulus.

4.2. Neural disarray and undersampling

The relative effects of neural disarray or undersampling are illustrated in Figures 10 (a,b), where D4 stimuli have been processed through jittered and/or sparse neural arrays respectively. In Fig. 10(a), when the neural array is irregularly sampled as it would be in one version of disarray, the discrimination between a perfect and distorted D4 becomes impossible. This occurs for relatively small degrees of disarray. Similar results were obtained analytically by Wilson (1991) for several hyperacuity tasks.

In the case of undersampling, which is shown in Fig. 10(b), a similar difficulty occurs in the discrimination of the perfect from the distorted D4. This begins to arise when the Nyquist frequency of the sampling array approaches the peak spatial frequency of the D4 stimulus.

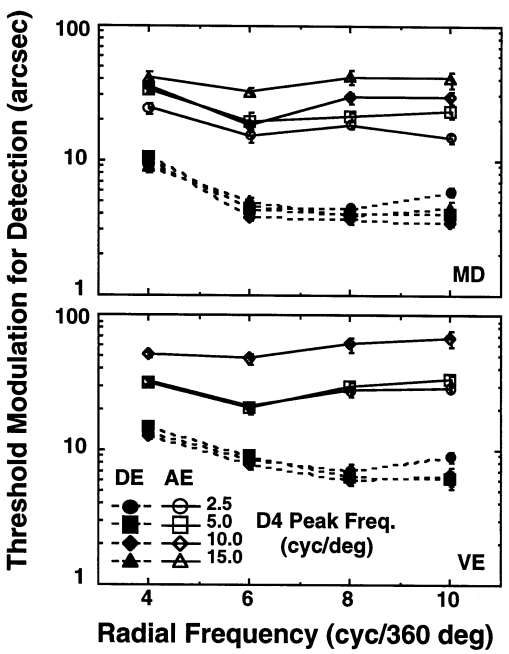

Fig. 5. The threshold modulation as a function of radial frequency with D4 peak spatial frequency as a parameter obtained from two subjects (MD and VE). The D4 peak frequencies used were 2.5 (circles), 5.0 (squares), 10 (diamonds) or 15 (triangles) cyc/°. Closed symbols are the results from the dominant eye, and open symbols are those from the amblyopic eye. Error bars indicate ±S.E.M. of at least five measurements.

5. Discussion

These results demonstrate that strabismic amblyopes exhibit abnormalities for detecting radial modulations. These abnormalities affect low as well as high radial frequencies to about the same degree (i.e. scale invariant). They are largely independent of the relationship of the spatial composition of the D4 stimulus to the amblyopic filtering loss and do not critically depend on the contrast of the D4 pattern. At suprathreshold levels, the performance of the amblyopic and fellow dominant eye is comparable.

Strabismic amblyopes are known to exhibit acuity deficits, reduced contrast sensitivity within their limited pass-band (Hess & Howell, 1977; Levi & Harwerth, 1977); and positional deficits (Bedell & Flom, 1981; Levi & Klein, 1982, 1983; Fronius & Sireteanu, 1989; Hess & Holliday, 1992; Demanins & Hess, 1996). Are the deficits measured here dependent upon any of these?

Since the D4 stimuli were always within the passband of the amblyopic visual system, it is unlikely that reduced acuity per se could explain our findings. Similarly, reduced contrast sensitivity within the amblyopic passband is an unlikely cause because not only is this task relatively independent of contrast above 15% (Wilkinson et al., 1998) but also our filtering simulation shows that it is relatively resistant to neural filtering. This is because the spatial composition of the radial modulations is well below that of the D4 pattern.

It is a more difficult task to dismiss positional uncertainty as a possible cause of the present deficits, especially since both deficits show a high degree of scale invariance (Hess & Holliday, 1992) and the results of a previous study on local shape detection implicated positional uncertainty as a possible cause (Pointer & Watt, 1987). Our feeling at this stage is that there is not as close a relationship between the magnitude of the D4 and positional deficits and for them to have a common cause. First, the present task, unlike that of a previous study (Pointer & Watt, 1987) has a global shape aspect to it which differs from a more local measure of positional uncertainty and there is evidence that a more global mechanism underlies performance on this task (Wilson et al., 1997; Wilkinson et al., 1998; Wang et al., 1998). This comes from a number of pieces of evidence. On the one hand, it has been shown that neither of the two candidate local measures (orientation and curvature) can explain performance (Wilson et al., 1997; Wilkinson 1998). On the other hand, performance depends on the phase of the modulation (i.e. global shape), the number of cycles of modulation and on how the modulation cycles are spatially arranged (Wang et al., 1998). Second, for a few (i.e. five) of these subjects we have positional measures for Gabors of approximately the same spatial characteristics as the D4 patterns and there is no signifi-

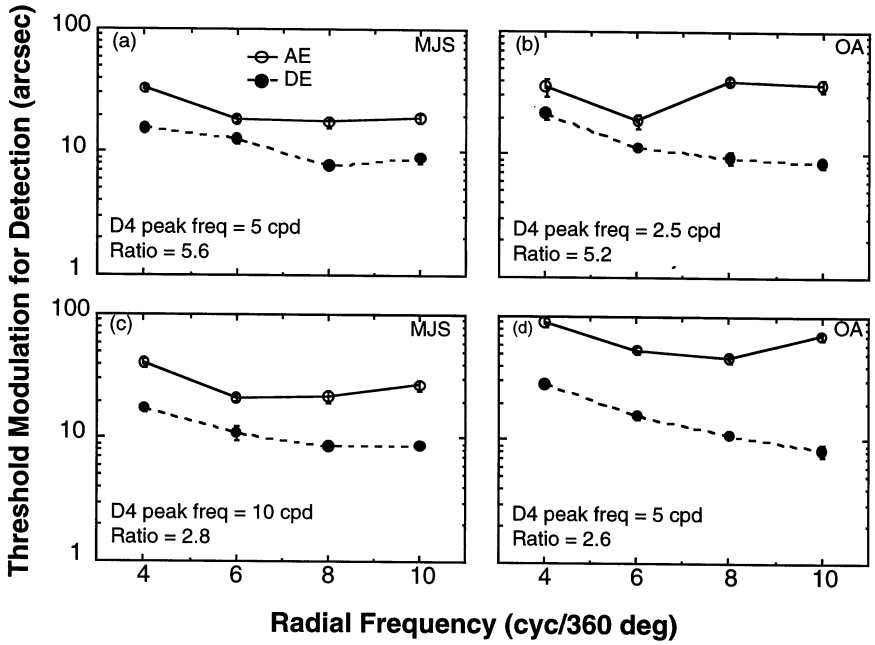

Fig. 6. Comparison of detection threshold for two subjects. (a, c) and (b, d): the subjects' grating detection acuities were about 5 times higher than the D4 peak spatial frequencies used; (a) and (b): the subjects' grating detection acuities were about 2.5 times higher than the D4 peak spatial frequencies; (c) and (d). Closed circles are the results from the dominant eye, and open circles are those from the amblyopic eye. Error bars indicate ±S.E.M. of at least three measurements.

cant correlation ($r = 0.48$—not significantly different from zero for the number tested) between the deficits for D4 distortion detection and positional uncertainty (see Table 2). One would need a much larger sample to be definitive on this issue.

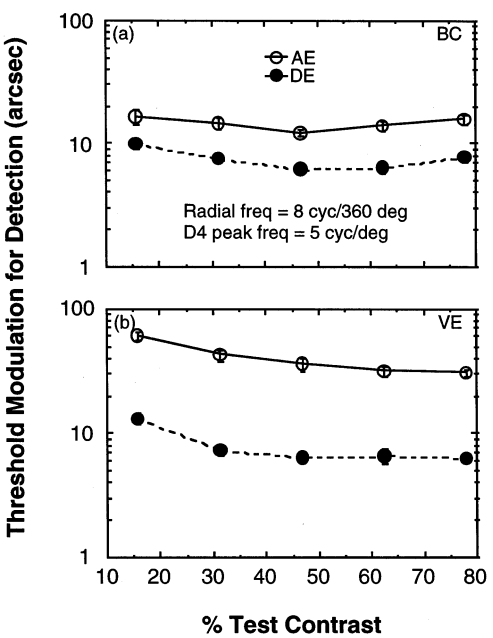

Fig. 7. The effect of stimulus contrast on the detection threshold for radial frequency modulation. The peak spatial frequency of the circular D4 contours was 5 cyc/°. The mean radius was 0.5°. The radial frequency was 8 cyc/360°. Closed circles are the results from the dominant eye, and open circles are those from the amblyopic eye. Error bars indicate ±S.E.M. of at least three measurements.

5.0.1. Possible cause

There has been a debate for some time concerning whether the deficits for spatial position in strabismic amblyopia are due to fewer cells (the undersampling hypothesis (Levi & Klein, 1982, 1986; also see Wilson, 1991) or a disordered mapping (the neural disarray hypothesis Hess, Campbell & Greenhalgh, 1978; Hess, 1982). Although the model simulations show that both types of loss could produce the detection abnormality observed here for D4 patterns, it is unlikely that undersampling of just high spatial frequency filters (Sharma, Levi & Coletta, 1997) is the cause because its effects would only be evident when the peak spatial frequency of the D4 pattern was close to the Nyquist limit. Not only did we ensure that the peak frequency of the D4 pattern was well below the amblyopes grating acuity but also we show that when the ratio of the grating acuity/peak D4 spatial frequency was high, that is when the stimulus is well below the acuity limit (the highest ratio tested was 8.4, subject BC), the abnormality for radial modulations did not disappear. If the deficit in amblyopia was limited to undersampling by high spatial frequency filters then one would not expect to find reduced modulation sensitivity for D4 stimuli of low peak spatial frequency. On the other hand if one considers undersampling within the context of different populations of scaled detectors, to account for the

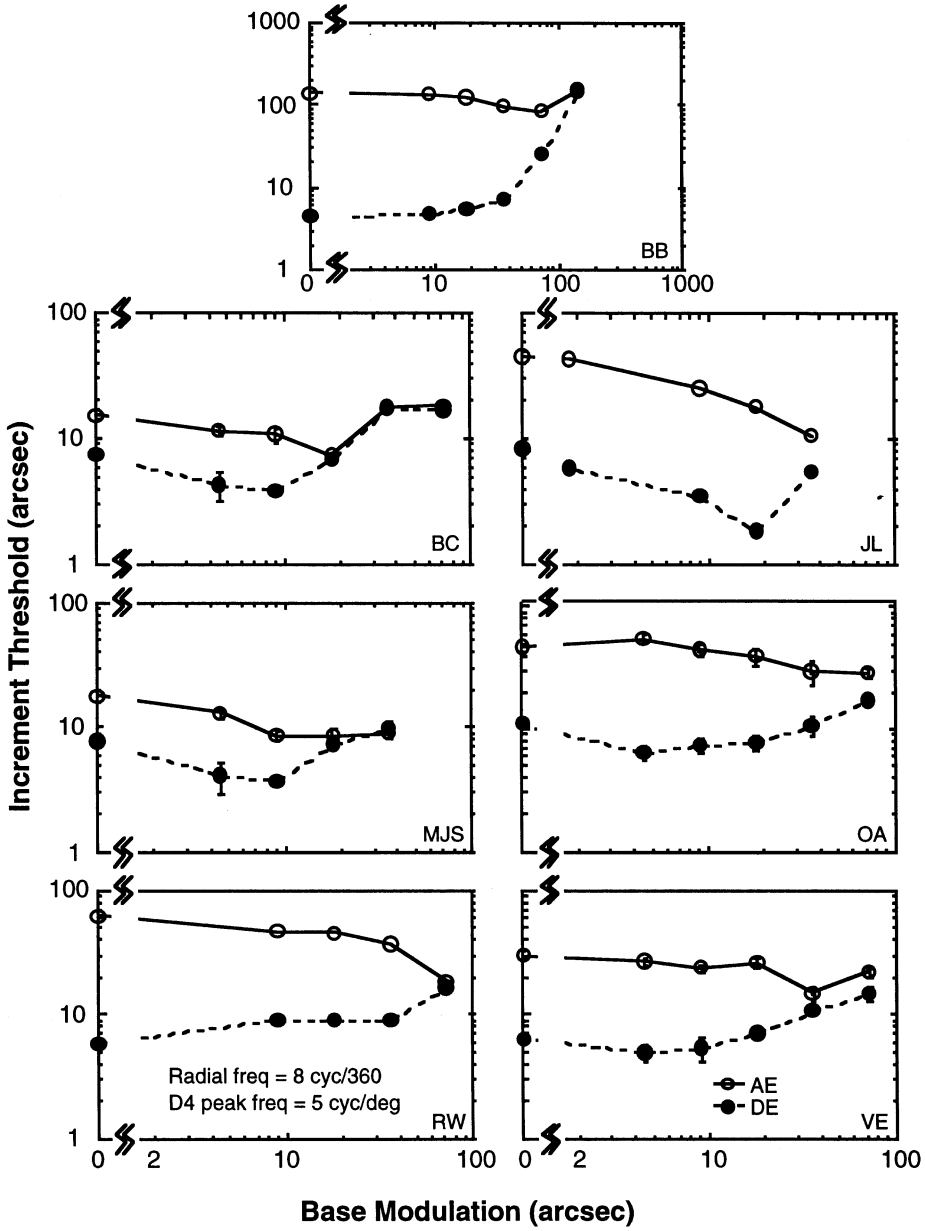

Fig. 8. Increment threshold for discriminating deformation of circular D4 contours as a function of pedestal modulation obtained from seven strabisrnic amblyopes. The peak spatial frequency of the circular D4 contours was 5 cyc/°. The mean radius was 0.5°. The radial frequency was 8 cyc/360°. Closed circles are the results from the dominant eye, and open circles are those from the arnblyopic eye. Error bars indicate ± S.E.M. of at least three measurements.

present results one would need to postulate that any undersampling occurred at all scales (Wilson, 1991). There has been a recent suggestion that the undersampling occurs at a stage beyond the early linear filters where there is postulated to be a more feature-based representation (Levi & Klein, 1996; Wang et al., 1998). If we assume this to be true, for the same reasons as described above, one would expect deficits at high radial frequencies which are close to the sampling limit and normal performance at low radial frequencies which are well below the sampling limit. This was not found to be the case.

Furthermore, the suprathreshold results suggest that the radial frequency deficit is additive rather than multiplicative (i.e. a parallel displacement of the curves in Fig. 8 describing normal and amblyopic performance as a function of base modulation) in nature; the discrimination curves for the dominant and fellow amblyopic eyes comes together in the high base or pedestal modulation range. By analogy with ideal observer noise analysis, this is consistent with there being a raised level of intrinsic noise of some kind in the amblyopic visual system restricting performance as a result of, for example, neural disarray. This would disrupt the encoding of

stimuli of low amplitude modulations but once the stimulus base modulation was large relative to the noise caused by the intrinsic disarray, its effect would diminish and eventually disappear. It is not consistent with reduced 'sampling efficiency' which would result in a multiplicative effect which in turn would be reflected in the curves in Fig. 8 (note, log/log plot) remaining parallel at high base modulations. Any loss in encoded amplitude as a result of reduced sampling will remain a constant fraction of the base modulation amplitude.

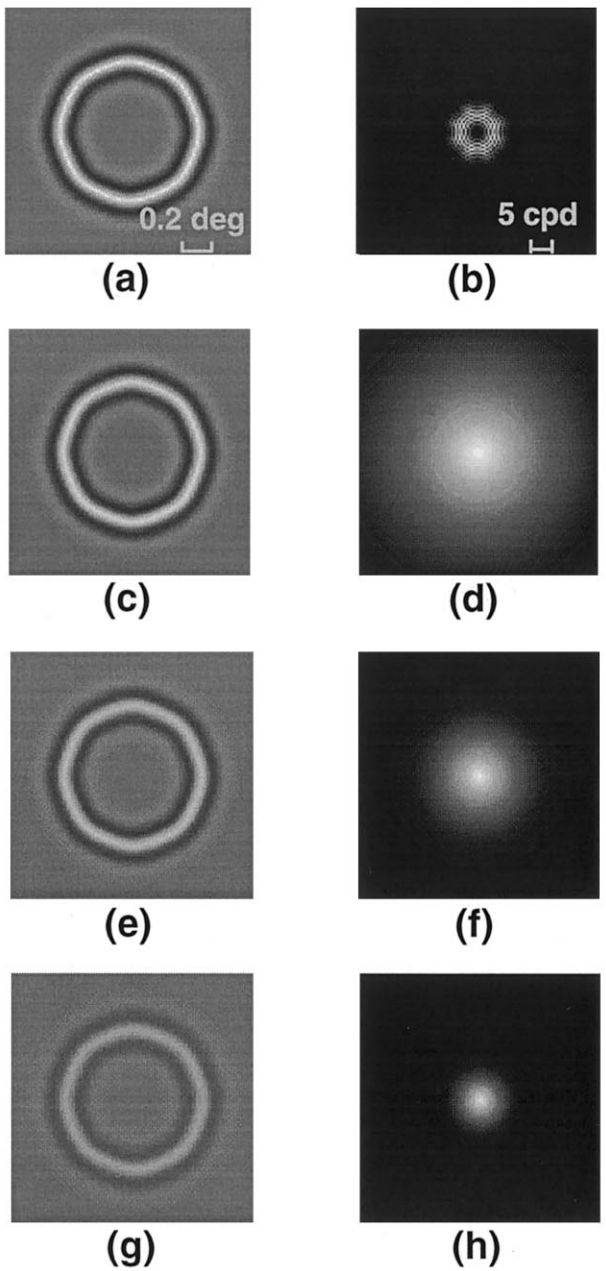

Fig. 9. Demonstration of the effect of spatial filtering. (a) deformed circular D4 contour, and (b) is its spectrum; (a) was filtered by three Gaussian filters (d, f, h) with different spatial frequency constants (cut-offs) of 20, 10, or 5 cyc/°, respectively; (c, e, g) show the corresponding filtered images.

In short, undersampling of a purely spatial nature or indeed reduced sampling, be it at an early or late stage in visual processing does not form an adequate explanation for the present results. Neural disarray at some stage in visual processing is a possible explanation for the present findings. We are not suggesting that there is no undersampling in the amblyopic visual system. Indeed we feel that this is likely at the highest spatial frequencies (Chino et al., 1983; Crewther & Crewther, 1990). What we are saying is that the current notion of undersampling (Levi & Klein, 1982, 1986), unless it is extended to be of a scale invariant nature, cannot be limiting performance in the lower spatial frequency range relevant to the processing of everyday images and in particular the radially modulated D4 stimuli used here.

5.0.2. Site of the abnormality

This task is believed to involve global shape and require the integration of large scale oriented filters (Wilson et al., 1997; Wilkinson et al., 1998; Wang et al., 1998). On the basis of what is known of the physiology of extrastriate areas (Foster, Gaska, Nagler & Pollen, 1985; Gallant et al., 1993, 1996), it is tempting to postulate that this task is accomplished beyond V1, in extrastriate areas where receptive field are not only larger but also have a polar arrangement. Even if it is true that an extrastriate area underlies performance on this task, it still may be that the ultimate limitation in amblyopia is downstream in V1.

Acknowledgements

This work was supported by the Canadian MRC (MT10818). We are grateful to all our subjects especially JL and BB.

Appendix A. Modeling of spatial filtering and neural sampling

A.1. Spatial filtering

The effect of spatial filtering on circular D4 patterns was studied using low-pass filters with different cut-off spatial frequencies. The amplitude of the low-pass filter was a circular Gaussian, as represented by the following equation:

$$G = \exp\left(-\frac{f_x^2 + f_y^2}{\sigma^2}\right) \quad \text{(A1)}$$

where f_x end f_y are the spatial frequency coordinates; σ is spatial frequency constant which defines the cutoff frequency of the low-pass filter. Spatial filtering process was done in the frequency domain. The spectrum of a

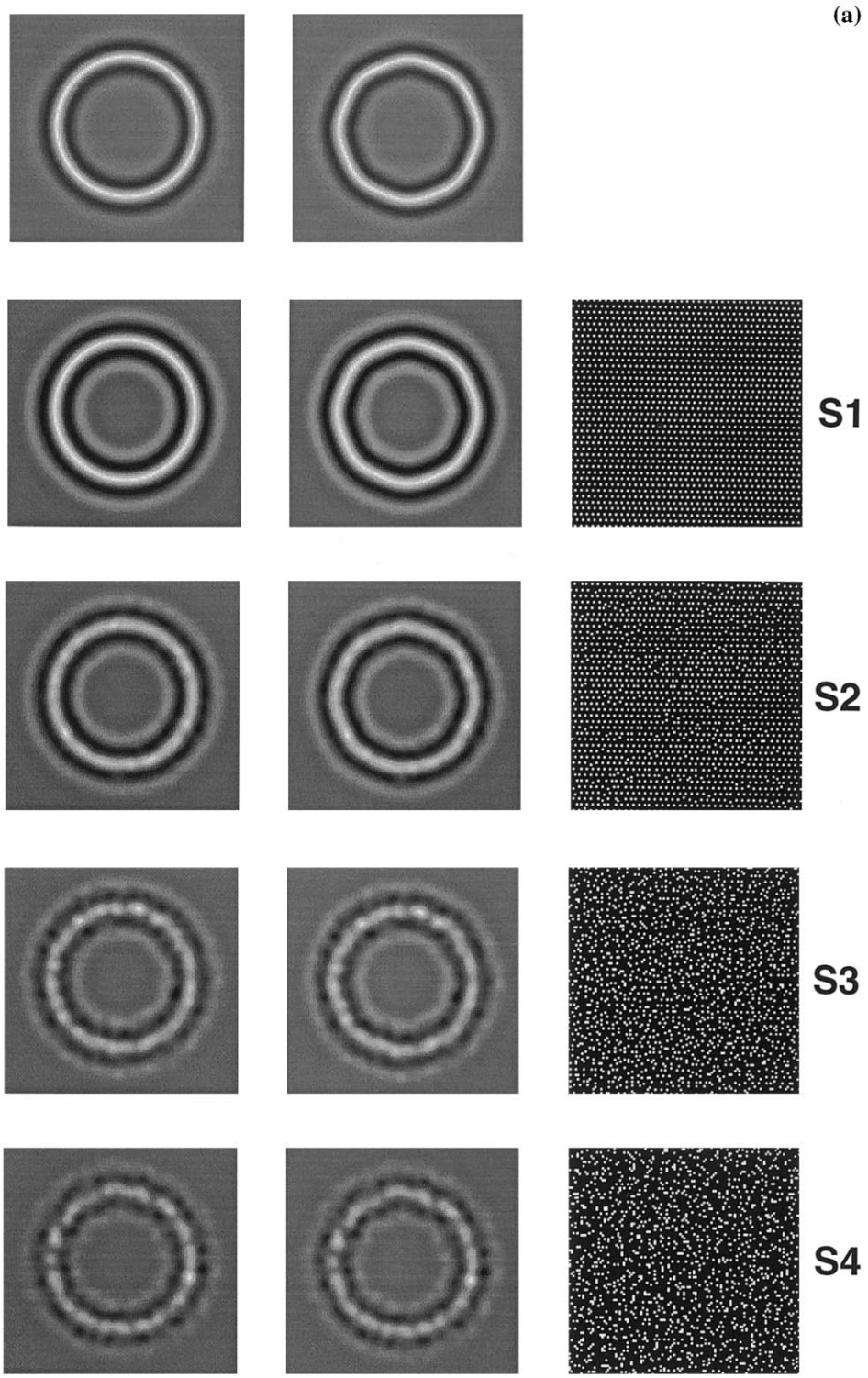

Fig. 10(a). Demonstration of the effect of irregular sampling. Top row shows an unmodulated circular D4 (left) and a modulated circular D4 with 1% of modulation (right). The D4 peak frequency is 5 cyc/°. Right column shows the sampling mosaic used. The initial sampling array is hexagonal, and its nominal Nyquist limit is 13.6 cyc/°. The irregular sampling was induced by jittering the regular sampling position with Gaussian noise. The S.D. of the Gaussian noise was represented by percent separation between samples, and was 0, 10, 25, and 50% for S1, S2, S3, and S4, respectively. The corresponding reconstructed images by DOG sampling-filtering are shown in the left two columns.

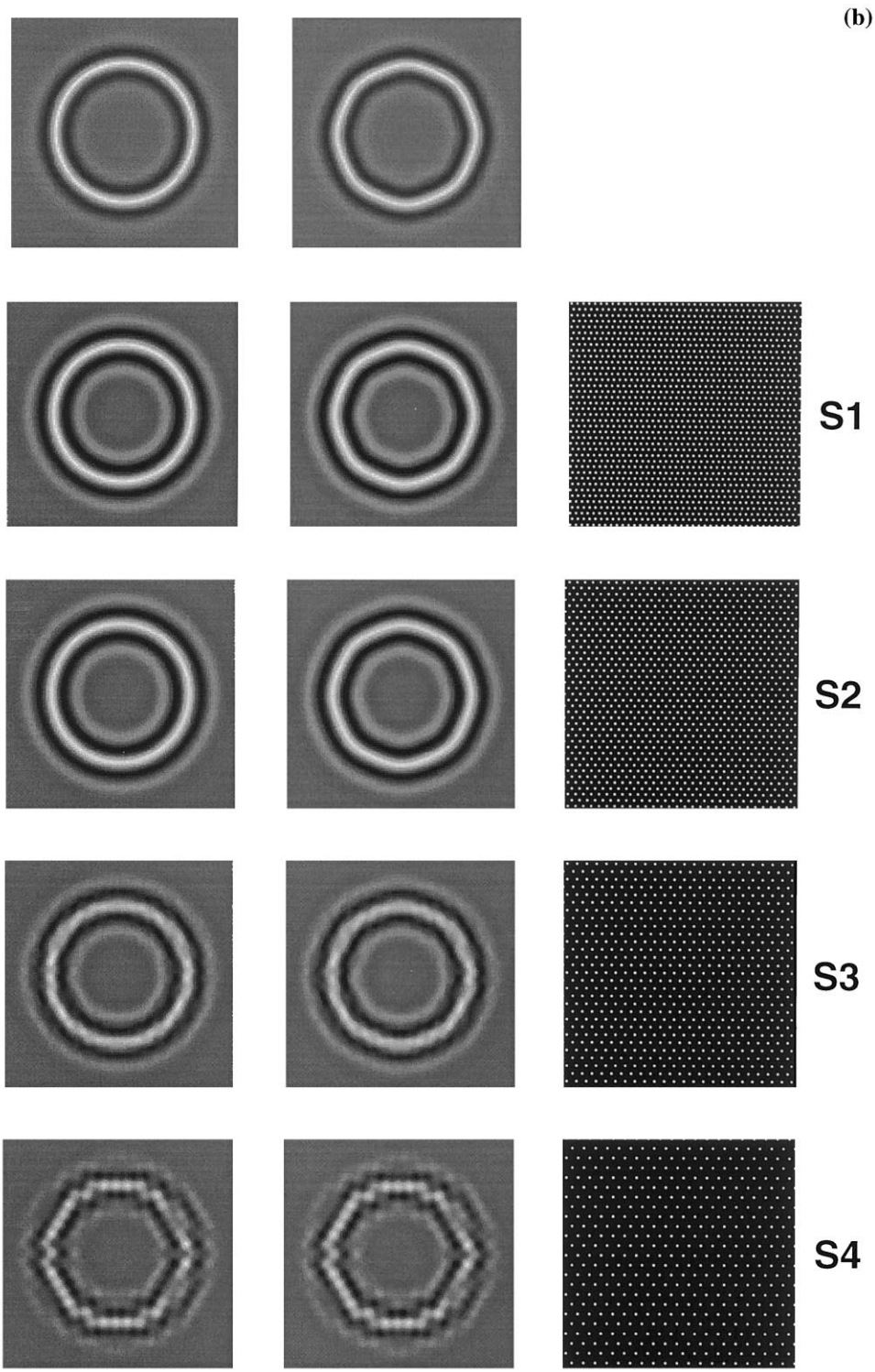

Fig. 10(b). Demonstration of the effect of 'undersampling' (or less neurons). Top row shows an unmodulated circular D4 (left) and a modulated circular D4 with 1% of modulation (right). The D4 peak frequency is 5 cyc/°. Right column shows the regular hexagonal sampling mosaic used. The nominal Nyquist limits of the sampling arrays are 13.6, 10.2, 8.2 and 6.8 cyc/° for S1, S2, S3 and S4, respectively. The corresponding reconstructed images by DOG-sampling-filtering are shown in the left two columns.

circular D4 pattern was first computed using the Fourier transform. Then the amplitude spectrum of a D4 pattern was multiplied by the amplitude of a Gaussian low-pass filter, while the phase of D4 pattern was unchanged. The filtered image was obtained by taking the inverse Fourier transform of the spectral product.

Table 2
Comparison of average D4 distortion detection and positional uncertainty deficits for five subjects

Subject	Average D4 distortion detection threshold ratios (D4 peak $sf = 5.0$ cyc/°)	Positional uncertainty ratios (Gabor $sf = 5.2$ cyc/°)
MJS	1.86	2.12
MS	1.98	2.89
OA	4.81	11.1
SA	6.22	4.20
VE	3.66	1.83

The D4 peak spatial frequency (sf) is 5 cyc/° and the ratio of dominant and amblyopic eye results at radial frequencies of 4,6,8,and 10 cyc/360° are averaged. The ratio of positional thresholds for the dominant and amblyopic eyes for Gabors with a spatial frequency of 5.2cyc/° are considered here (Demanins & Hess, 1996).
Linear regression: $y = 2.66 + 0.23x$.
$R = 0.48$.

A.2. Neural sampling

Sampling arrays with different amount of irregularity and Nyquist limits were created for modeling the effects of irregular sampling/disarray and undersampling on circular D4 patterns. The sampling array was based on a hexagonal lattice with spacing constant S between sample points. Irregularity of the array was introduced by displacing each point vertically and horizontally by a random amount (Wang, 1996). This spatial jitter was achieved by adding a different, independent sample from a Gaussian noise source (mean = 0; S.D. = σS) to the x- and y-coordinates of each point. The degree of irregularity in the sampling array was determined by parameter σ, which is the S.D. of the noise in units of the spacing constant S. The nominal Nyquist limit of an irregular sampling array, f_{NL} is defined as:

$$f_{NL} = \frac{1}{S\sqrt{3}} \tag{A2}$$

The spatial sampling process was implemented by multiplying a circular D4 pattern by a sampling array. Since postreceptoral processes were modeled here, instead of point-sampling, each sample location was weighted by a normalized, balanced DOG function which is represented by the following equation

$$\mathrm{DOG} = a \exp\left(-\frac{x^2 = y^2}{\sigma_p^2}\right) - b \exp\left(-\frac{x^2 = y^2}{\sigma_N^2}\right) \tag{A3}$$

The coefficients a and b and space constants σ_P^2 and σ_N^2 must satisfy the following relationship so that DOG is balanced and normalized:

$$a = b\frac{\sigma_N^2}{\sigma_p^2} \quad \text{and} \quad a - b = 1 \tag{A4}$$

In our modeling, $6_N = 1.56_p$ i.e. DOGs have positive centers.

For a given D4 pattern, 6_p was chosen so that the DOG weighting function was tuned to the D4 stimulus (i.e. the center of DOG matches that of D4). The DOG function was centered at each sample point. The sampled image value at each point was the sum of the products of the balanced DOG and the D4 pattern. The reconstructed image was obtained by convolving the sampled image with the same balanced DOG filter used for sampling.

The computation was done in MATLAB.

Acknowledgement

We are grateful for support from Canadian MIRC to RFH (MI108-18).

References

Bedell, H. D., & Flom, M. C. (1981). Monocular spatial distortion in strabismic amblyopia. *Investigative Ophthalmology and Visual Science*, *20*, 263–268.

Bedell, H. E., Flom, M. C., & Barbeito, R. (1985). Spatial aberrations and acuity in strabismus and amblyopia. *Investigative Ophthalmology and Visual Science*, *26*, 909–916.

Brainard, D. H. (1997). The psychophysics toolbox. *Spatial Vision*, *10*, 433–446.

Chino, Y. M., Shansky, M. S., Jankowski, W. L., & Banser, F. A. (1983). Effects of rearing kittens with convergent strabismus on development of receptive-field properties in striate cortex neurons. *Journal of Neurophysiology*, *50*, 265–286.

Crewther, D. P., & Crewther, S. G. (1990). Neural site of strabismic amblyopia in cats: spatial frequency deficit in primary cortical neurons. *Experimental Brain Research*, *79*, 615–622.

Demanins, R., & Hess, R. F. (1996). Positional loss in strabismic amblyopia-interrelationship of alignment threshold, bias, spatial scale and eccentricity. *Vision Research*, *36*, 2771–2794.

Foster, K. H., Gaska, J. P., Nagler, M., & Pollen, D. A. (1985). Spatial and temporal frequency selectivity of neurones in visual cortical areas V1 and V2 of the macaque monkey. *Journal of Physiology*, *365*, 331–363.

Fronius, M., & Sireteanu, R. (1989). Monocular geometry is selectively distorted in the central visual field of strabismic amblyopes. *Investigative Ophthalmology and Visual Science*, *30*, 2034–2044.

Gallant, J. L., Braun, J., & Van Essen, D. C. (1993). Selectivity for polar, hyperbolic, and Cartesian gratings in macaque visual cortex. *Science*, *259*, 100–103.

Gallant, J. L., Connor, C. E., Rakshit, S., Lewis, J. W., & Van Essen, D. C. (1996). Neural responses to polar, hyperbolic, and Cartesian gratings in area V4 of the macaque monkey. *Journal of Neurophysiology*, *76*, 2718–2739.

Hess, RF, & Holliday, I. E. (1992). The spatial localization deficit in amblyopia. *Vision Research*, *32*, 1319–1339.

Hess, R. F., & Howell, E. R. (1977). The threshold contrast sensitivity function in strabismic amblyopia: Evidence for a two type classification. *Vision Research*, *17*, 1049–1055.

Hess, R. F. (1982). Developmental sensory impairment: amblyopia or tarachopia? *Human Neurobiology*, *1*, 17–29.

Hess, R. F., Campbell, F. W., & Greenhalgh, T. (1978). On the nature of the neural abnormality in human amblyopia; neural aberrations and neural sensitivity loss. *Pflugers Archiv European Journal of Physiology*, *377*, 201–207.

Hess, R. F., McIlhagga, W., & Field, D. J. (1997). Contour integration in strabismic amblyopia: the aufficiency of an explanation based on positional uncertainty. *Vision Research*, *37*, 3145–3161.

Lagreze, W. D., & Sireteanu, R. (1991). Two-dimensional spatial distortions in human strabismic amblyopia. *Visual Research*, *31*, 1271–1288.

Levi, M., & Harwerth, R. S. (1977). Spatio-temporal interactions in anisometropic and strabismic amblyopia. *Investigative Ophthalmology and Visual Science*, *16*, 90–95.

Levi, D. M., & Klein, S. (1982). Hyperacuity and amblyopia. *Nature*, *298*, 268–270.

Levi, D. M., & Klein, S. A. (1983). Spatial localization in normal and amblyopic vision. *Vision Research*, *23*, 1005–1017.

Levi, D. M., & Klein, S. A. (1986). Sampling in spatial vision. *Nature*, *320*, 360–362.

Levi, D. M., & Klein, S. A. (1996). Limitations on position coding imposed by undersampling and univariance. *Vision Research*, *36*, 2111–2120.

Nachmias, J. (1981). On the psychometric function for contrast detection. *Vision Research*, *21*, 215–223.

Pelli, D. G. (1997). The VideoToolbox software for visual psychophysics: transforming numbers into movies. *Spatial Vision*, *10*, 437–442.

Pointer, J. S., & Watt, R. J. (1987). Shape recognition in amblyopia. *Vision Research*, *27*, 651–660.

Sharma, V., Levi, D. M., & Coletta, N. J. (1997). Sparse sampling in central vision of strabismic amblyopes. *Investigative Ophthalmology and Visual Science*, *38*, 108.

Wang, Y. Z. Filtering, sampling and aliasing in peripheral vision. Bloomington: Indiana University. PhD 1996, pp. 158–221.

Wang, Y.-Z., Hess, R. F., & Dakin, S. C. (1998). Judgements of circularity; local or global. *Invest. Opthal Vis. Sci. (Suppl) 39*(4) S847.

Wang, H., Levi, D. M., & Klein, S. A. (1998). Spatial uncertainty and sampling efficiency in amblyopic position acuity. *Vision Research*, *38*, 1239–1251.

Weibull, W. (1951). A statistical distribution function of wide applicability. *Journal of Applied Mechanics*, *18*, 292–297.

Wilson, H. R. (1991). Model of peripheral and amblyopic hyperacuity. *Vision Research*, *31*, 967–982.

Wilson, H. R., Wilkinson, F., & Asaad, W. (1997). Concentric orientation summation in human form vision. *Vision Research*, *37*, 2325–2330.

Wilkinson F., Wilson H.R., & Habak C. (1998). Detection and recognition of radial frequency patterns. Vision Research, *38*, 3555–3568.